

## The Domany-Kinzel cellular automaton: relaxation time, susceptibility and constrained dynamics

This article has been downloaded from IOPscience. Please scroll down to see the full text article.

1994 J. Phys. A: Math. Gen. 27 1

(<http://iopscience.iop.org/0305-4470/27/1/001>)

View [the table of contents for this issue](#), or go to the [journal homepage](#) for more

Download details:

IP Address: 171.66.16.68

The article was downloaded on 01/06/2010 at 21:16

Please note that [terms and conditions apply](#).

# The Domany–Kinzel cellular automaton: relaxation time, susceptibility and constrained dynamics

M L Martins†§, G F Zebende‡, T J P Penna‡ and C Tsallis§

† Departamento de Física, Universidade Federal de Viçosa, Viçosa, 36570-000, Minas Gerais, Brazil

‡ Instituto de Física, Universidade Federal Fluminense, Niterói, 24001-970, Rio de Janeiro, Brazil

§ Centro Brasileiro de Pesquisas Físicas, Rua Xavier Sigaud 150, Rio de Janeiro, 22290-180, Rio de Janeiro, Brazil

Received 26 July 1993

**Abstract.** We use Monte Carlo simulation to study new features of the (one-dimensional) Domany–Kinzel cellular automaton (CA). Considering the relaxation process of the ‘magnetization’ (the frozen–active order parameter) towards its equilibrium value, we measure its dynamical critical exponent  $z$ . Also, we investigate the effect of  $p_{11} \neq 0$  (non-vanishing external field conjugate to the magnetization) on the phase diagram and on the susceptibility. Finally, we introduce constraints in the evolution rule of the Domany–Kinzel CA and study the associated criticality (critical surfaces and universality classes).

## 1. Introduction

Cellular automata (CA) are totally discrete dynamical systems (discrete space, discrete time and discrete number of states) which provide simple models for a great number of problems in science. CA have frequently been used to model chemical reactions, crystal growth models, turbulence, neural networks, biological systems, or other nonlinear processes far from thermal equilibrium [1]. But it is not only the practicality in simulating differential equations, like fluid dynamics, that explain the recent great interest in CA. If the deep nature of spacetime turns out to be discrete, CA, and not only the traditional differential equations, could be a helpful description of the physical world.

In the CA context, the discrete space is represented by a regular lattice and with each site  $i$  of the lattice one associates a variable  $\sigma_i$  which can take  $k$  different values  $\sigma_i = 0, 1, \dots, k - 1$ . The CA time evolution is defined, at each time step, by local rules where the value  $\sigma_i$  at time  $t$  depends, in a deterministic or probabilistic way, on the state of the system at time  $t - 1$ . All the sites are simultaneously updated at each time step. Since its dynamics is not restricted to the usual Boltzmann weight and detailed balance, CA do not necessarily evolve (in the long time asymptotic limit) towards the standard thermal equilibrium.

The study of CA is a very interesting one because of their fascinating intrinsic dynamics. The attractors can present spatial and/or temporal modulations of various kinds (such as fractal or translationally invariant structures) as well as spatial and/or temporal chaos. Also, the time evolution towards the attractors often exhibits interesting types of sensitivity to the initial conditions (with or without damage spread) [2]. Finally, order parameters characterizing the various possible attractors (‘phases’) can be studied as well, thus enabling

the establishment of the CA phase diagram with all sorts of critical phenomena, critical exponents and universality classes. Various types of susceptibilities and relaxation times can be analysed as well.

In this paper, some of the above relevant properties (susceptibility, relaxation time and phase diagram for a constrained case) of the (one-dimensional) Domany–Kinzel CA are investigated in some detail, through Monte Carlo simulations. In these simulations we used, for each set of parameters defining the CA, a quite large number (typically up to 100) of random starting configurations where all states were equally probable. In section 2 we recall the model and its phase diagram. In section 3 the magnetization relaxation process towards its equilibrium value is studied. In section 4 we investigate the influence of a uniform external field (conjugate to the magnetization) on the phase diagram as well as on the susceptibility. Finally, in section 5 we introduce a constraint in the evolution rule of the CA and discuss the associated criticality (critical surface and universality classes). We draw a conclusion in section 6.

## 2. The Domany–Kinzel CA

Although  $d$ -dimensional (probabilistic) CA describe processes that might be far from equilibrium, they can frequently be mapped onto  $(d + 1)$ -dimensional statistical-mechanics models [3]. The corresponding spin model is, in general, anisotropic and involves multispin interactions and fields, with coupling constants related to the parameters (conditional probabilities) which specify the evolution rule of the CA. Therefore it is not surprising that even one-dimensional CA exhibit continuous phase transitions with universal critical exponents and scaling laws.

The one-dimensional CA considered by Domany and Kinzel [4] consists of a linear chain of  $N$  lattice sites ( $i = 1, 2, \dots, N$ ), with periodic boundary conditions. Each site has two possible states  $\sigma_i = 0, 1$ . The state of the system at time  $t$  is specified by the set  $\{\sigma_i\}$ . At the next time step, the state of a given site is  $\sigma_i(t + 1) = 0$  or 1 according to the conditional probabilities  $\{p(\sigma_{i-1}(t), \sigma_i(t) | \sigma_i(t + 1))\}$ , i.e.  $p(00/1)$ ,  $p(10/1)$ ,  $p(01/1)$  and  $p(11/1)$ . We shall study the isotropic case  $p(01/1) = p(10/1) \equiv p_1$ ,  $p(11/1) \equiv p_2$  and  $p(00/1) \equiv p_0$ . Naturally  $p(\sigma_{i-1}, \sigma_i/0) = 1 - p(\sigma_{i-1}, \sigma_i/1)$ . A possible application of this CA is to model catalysis in chemical reactions [5]. The Domany–Kinzel CA contains, as special cases, the problem of directed percolation and directed compact percolation [6, 7] on the square lattice.

Depending on the values of  $(p_1, p_2)$ , the  $t \rightarrow \infty$  asymptotic state is homogeneous with all sites 0 (frozen phase) or has a finite fraction of interchanging sites with value 1 (active phase). These two phases are connected through a continuous phase transition (characterized by universal critical exponents) as demonstrated in the original work of Domany and Kinzel. Recently, it has been shown numerically, on a generalized version which includes anisotropy, that the active phase splits, in fact, into two phases, only one of them being chaotic [8]. These numerical results received further confirmation by more extensive simulations [9], as well as through mean-field-like approximations [9, 10]. The complete phase diagram for the original, isotropic Domany–Kinzel CA is depicted in figure 1 [8].

The order parameters characterizing the three phases are the magnetization  $M$ , defined as the fraction of sites with value 1, and the normalized Hamming distance  $\Psi$ , defined as the fraction of sites that differ between two different initial configurations evolving under the same noise (i.e. the same random numbers sequence). In the chaotic phase, the automaton is sensitive to the initial conditions and an ‘initial damage’, created by randomly flipping a fraction  $p$  of the sites of a given configuration, spreads through the entire CA. Thus in the

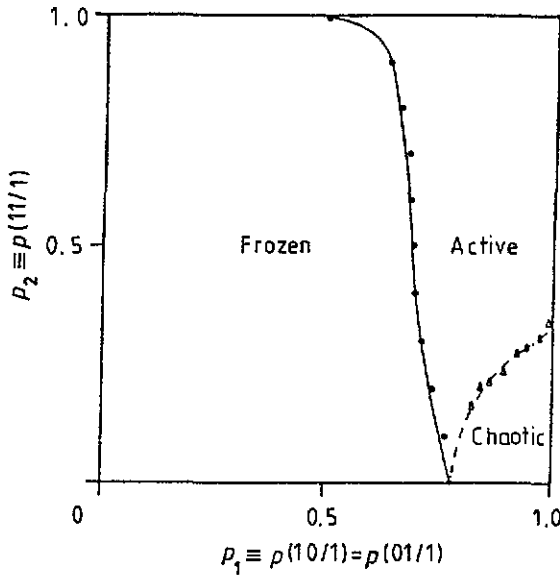


Figure 1.  $p(00/1) = 0$  and  $p(10/1) = p(01/1)$  (isotropic) phase diagram. The data correspond to simulations with 3200 sites; transients of 10 000 (3000) time steps were used for the frozen-active (active-chaotic) phase transitions. The damage was averaged over another 30 000 time steps.

frozen phase we have  $M = 0$  and  $\Psi = 0$ ; in the active phase  $M \neq 0$  and  $\Psi = 0$ ; and in the chaotic phase  $M \neq 0$  and  $\Psi \neq 0$ . Let us add that comparison between the present  $p_2 = 1$  results and those associated with the directed compact percolation must be done with care since it is not obvious that  $M$  is proportional to the order parameter introduced in [6, 7].

### 3. The time evolution of the magnetization

In the computational calculation of say the frozen-active critical surface, it is necessary to evolve the automaton until it reaches equilibrium, evaluating, at each time step, the order parameter  $M$ . So, the automaton evolves until there are no large fluctuations of the magnetization. The figures 2(a) and (b) show the order parameter  $M_t$  as a function of time for two sets of conditional probabilities which correspond to points in the frozen phase, respectively far from and near to the critical surface. The behaviour of the transient of  $M_t$  for a point which belongs to the non-frozen phase and which is far from the critical surface is shown in figure 2(c). We observe in figure 2 that the transient is longer near the critical surface than far from this surface; it is expected that the necessary time for the magnetization to reach equilibrium diverges on the critical surface in the thermodynamical limit ( $N \rightarrow \infty$ ).

As one can see from figure 2, the magnetization shows an exponential decay towards its equilibrium value according to the formula

$$M_t - M_\infty \sim e^{-t/\tau} \quad (1)$$

where, strictly speaking,  $M_\infty \equiv \lim_{t \rightarrow \infty} \lim_{N \rightarrow \infty} M_t$  (not to be confused with  $\lim_{N \rightarrow \infty} \lim_{t \rightarrow \infty} M_t$ , which generically vanishes, as pointed out by Carter [11]). Near the critical surface we expect that the characteristic relaxation time  $\tau$  obeys the power law

$$\tau \simeq |p_1 - p_{1c}|^{-z}. \quad (2)$$

However, for computational simplicity, instead of determining  $\tau$  (and its exponent  $z$ ) from the exponential decay of the magnetization, we measure directly the total time  $\tau^*$

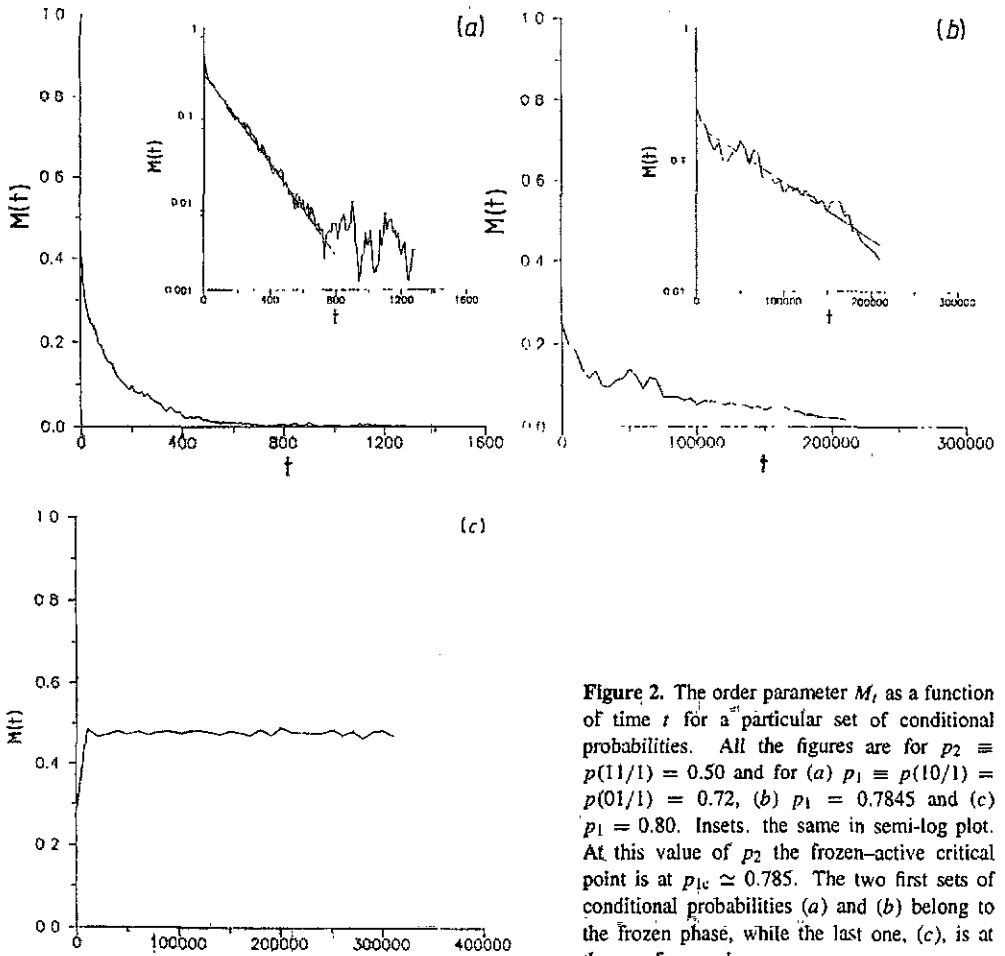


**Figure 2.** The order parameter  $M_t$  as a function of time  $t$  for a particular set of conditional probabilities. All the figures are for  $p_2 \equiv p(11/1) = 0.50$  and for (a)  $p_1 \equiv p(10/1) = p(01/1) = 0.72$ , (b)  $p_1 = 0.7845$  and (c)  $p_1 = 0.80$ . Insets: the same in semi-log plot. At this value of  $p_2$  the frozen-active critical point is at  $p_{1c} \approx 0.785$ . The two first sets of conditional probabilities (a) and (b) belong to the frozen phase, while the last one, (c), is at the non-frozen phase.

necessary for the magnetization to reach its equilibrium value. Since  $\tau^*$  is proportional to  $\tau$ , equation (2) leads to

$$\tau^* \approx |p_1 - p_{1c}|^{-z} \quad (3)$$

at fixed  $p_2$ . This expression defines the relaxation time critical exponent  $z$  for this order parameter. In figure 3 we present a typical log-log plot of  $\tau^* \times |p_1 - p_{1c}|$ . As a result of these simulations we find  $z = 1.0 \pm 0.03$ . Since these simulations are in fact quite large ones (involving up to  $10^6$  time steps in a system with 12 800 sites), we believe that the exact value might be  $z = 1$ .

There is also a similar relaxation process associated with the normalized Hamming distance  $\Psi$ , the order parameter of the active-chaotic phase transition. This process can possibly be characterized by a distinct value for the critical exponent  $z$ .

#### 4. The effect of a uniform external 'field'

If one considers  $p_0 \equiv p(00/1) = 0$ , it is obvious that, if the configuration of the system is zero (i.e. all the sites have state 0) at time  $t$ , it will remain zero for all subsequent time

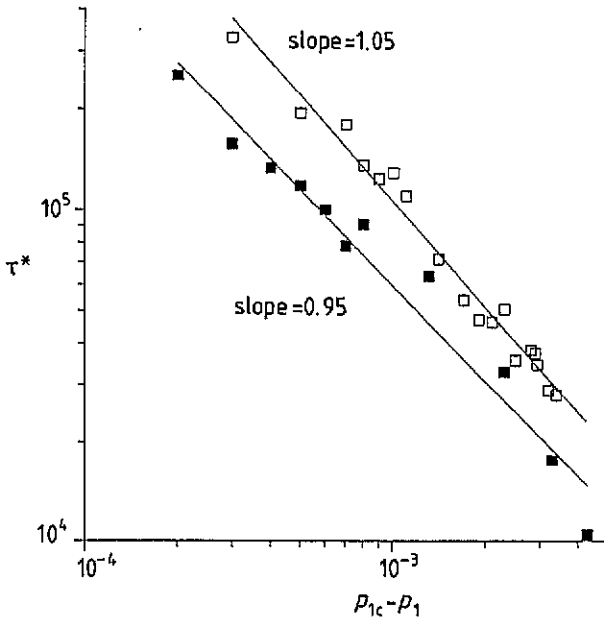


Figure 3. Log-log plot of  $\tau^*$  versus  $(p_{1c} - p_1)$  in the isotropic case. The data correspond to simulations with 3200 (■) and 12 800 (□) sites. The full lines are guides to the eye.

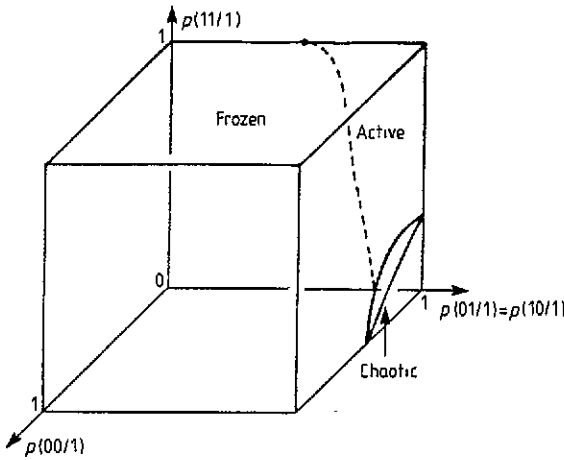


Figure 4. Phase diagram for the isotropic case ( $p(10/1) = p(01/1)$ ) and arbitrary  $p_0 \equiv p(00/1)$ .

steps ( $M_\infty = 0$ ). On the other hand, if  $p_0 \neq 0$  and the system is at the configuration zero at time  $t$ , it will acquire a non-vanishing fraction of sites with states different from zero ( $M_\infty \neq 0$ ), at subsequent time steps. The probability  $p_0$  is, consequently, analogous to an external field in ferromagnets, which destroys the phase transition. This is the reason for only considering legal rules ( $p_0 = 0$ ) in the Domany–Kinzel CA when we investigate the frozen–active critical surface.

If we now consider  $p_0 \neq 0$ , the frozen–active critical surface disappears but the active–chaotic one remains, as shown in figure 4. We can also study the associated susceptibility

$$\chi \equiv \left. \frac{\partial M}{\partial p_0} \right|_{p_0=0} \quad (4)$$

We calculate this derivative numerically. Although this method is not very accurate, we used it because of the lack of a fluctuation–dissipation-like relation valid in the frozen

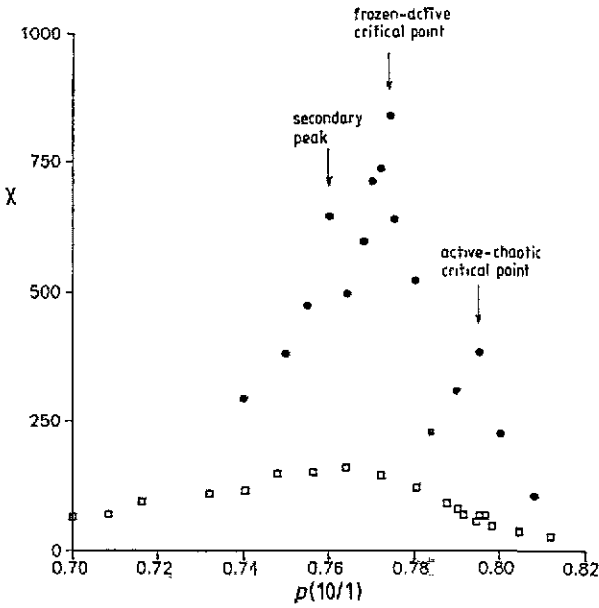


**Figure 5.** Susceptibility  $\chi = \partial M / \partial p_0 |_{p_0=0}$  obtained numerically for  $p(11/1) = 0.1$ . The data used to take the numerical derivative of  $M$  corresponds to  $p_0 \simeq 10^{-4}$  ( $\square$ ) and  $p_0 \simeq 10^{-5}$  ( $\bullet$ ). The system consists of 3200 sites.

phase. In figure 5 we show the susceptibility for  $p_2 = 0.1$ . This curve shows, besides the expected tendency towards divergence at the frozen-active critical surface, a small peak at the chaotic-active critical surface. Although hard to understand, we observe systematically a secondary peak at the left side of the central one; in order to decide whether this unexpected peak is not due to statistical fluctuations, more simulations (and for other values of  $p_0$ ) would be necessary. It should be noted that more extensive simulations are necessary in order to calculate the critical exponent associated with the susceptibility divergence.

## 5. Constrained dynamics

The results we have presented up to now have been obtained by using *independent* random numbers for updating *each* one of the  $N$  sites at *each* time  $t$ . Let us now generalize this by introducing constraints in the Domany-Kinzel CA. The constraints we shall consider consist of using, at a given time step, the *same* random numbers to update  $n$  ( $1 \leq n \leq N$ ) neighbouring sites (the same set of groups of  $n$  sites each for all times). The  $n = 1$  model recovers the original CA; the  $n = N$  is an extreme case for which a single random number is used for updating the entire generation. The phase diagram for various  $n$  is shown in figure 6. In the  $n = N \rightarrow \infty$  limit, the  $p_0 = 0$  phase diagram exhibits a frozen phase almost everywhere since the frozen-active and the active-chaotic critical lines have collapsed onto the  $p_2 = 1$  line and/or onto the  $p_1 = 1$  line. This fact cannot be considered as surprising since, in the  $n = N \rightarrow \infty$  limit, the system becomes one-dimensional-like in spacetime because the space randomness disappears (whereas it is two-dimensional for finite  $n$  and  $N \rightarrow \infty$ ). Moreover, we can see from this phase diagram (figure 6(a)) that the frozen phase area  $A_f$  tends to unity whereas the active area  $A_a$  as well as the chaotic area  $A_c$  tend to zero when  $n$  increases from 1 to  $\infty$ ; in addition, we verify that the ratio  $A_a/A_c$  decreases with increasing  $n$ . Hence, tendency towards a 'totalitarian' limit (*same* random number for *all* the elements of a given generation) decreases chaos, but decreases even more (certain types of) activity!

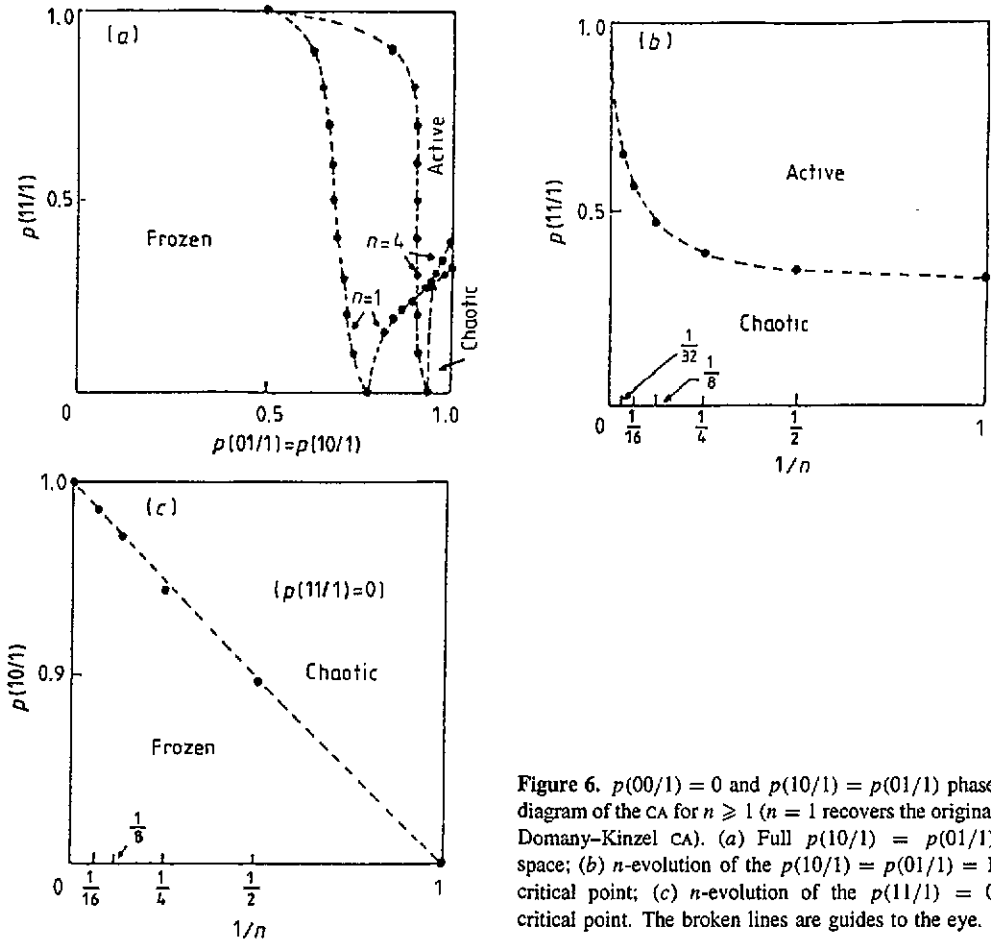


Figure 6.  $p(00/1) = 0$  and  $p(10/1) = p(01/1)$  phase diagram of the CA for  $n \geq 1$  ( $n = 1$  recovers the original Domany–Kinzel CA). (a) Full  $p(10/1) = p(01/1)$  space; (b)  $n$ -evolution of the  $p(10/1) = p(01/1) = 1$  critical point; (c)  $n$ -evolution of the  $p(11/1) = 0$  critical point. The broken lines are guides to the eye.

An important question remains to be answered: do the constraints we have introduced in the CA modify the known universality classes of this model? To investigate this we studied the magnetization critical exponent  $\beta$  as a function of the constraints range  $n$ . Our results are shown in figure 7 and indicate that the universality classes in the constrained and in the original cases are the *same*, except for  $n = N \rightarrow \infty$ . This fact cannot be considered as completely surprising since each block of  $n$  constrained sites behaves, in some sense, at criticality, as if it was a unique effective site of the original Domany–Kinzel CA.

## 6. Conclusions

We have studied, by Monte Carlo simulation, some important properties of the isotropic (one-dimensional) Domany–Kinzel cellular automaton. A study of the relaxation process towards equilibrium of the frozen–active phase transition order parameter was done and its relaxation time exponent was determined. The influence of the conditional probability  $p_0 \equiv p(00/1)$  was analysed. Although this probability is the field conjugate to the magnetization, it does not destroy the active–chaotic phase transition. Considering  $p_0 \neq 0$  we present preliminary results about the susceptibility for this CA, which, besides the tendency towards divergence at the frozen–active critical surface, exhibits sensitivity to the



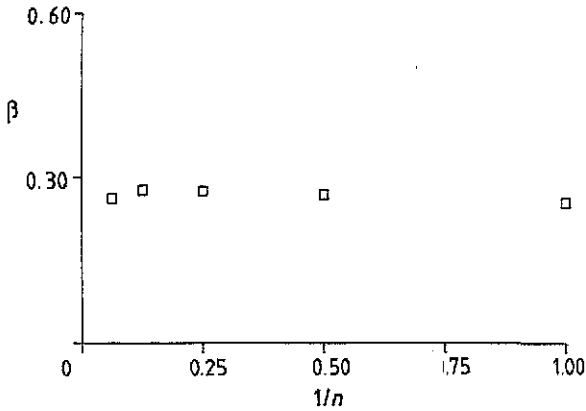


Figure 7. Magnetization critical exponent  $\beta$  as a function of the constraints range  $n$  for  $p(1/1) = 0.7$ . The data correspond to simulations with 3200 or 6400 sites; transients of 50 000 time steps were used for the frozen-active phase transition. The magnetization was averaged over another 100 000 time steps.

active-chaotic transition. Also, we have generalized the Domany-Kinzel cellular automaton in the sense that one updates a block of  $n$  ( $1 \leq n \leq N$ ) sites using the same random number. Then we calculated the  $n$ -evolution of the phase diagram. Finally, we found that the universality classes for the constrained case are the same as those of the original Domany-Kinzel CA.

### Acknowledgments

One of the authors CT acknowledges fruitful discussions with J W Essam. MLM would like to acknowledge the partial support given to this work by the Fundação de Amparo à Pesquisa do Estado de Minas Gerais (FAPEMIG).

### References

- [1] Farmer D, Toffoli T and Wolfram S (eds) 1984 *Cellular Automata in Physica* **10D**  
Wolfram S 1986 *Theory and Applications of Cellular Automata* (Singapore: World Scientific)
- [2] Tsallis C 1992 *Condensed Matter Theories* ed L Blum (New York: Plenum)
- [3] Rujan P 1987 *J. Stat. Phys.* **49** 139  
Georges A and Doussal P Le 1989 *J. Stat. Phys.* **54** 1011
- [4] Domany E and Kinzel W 1984 *Phys. Rev. Lett.* **53** 447  
Kinzel W 1985 *Z. Phys.* **B 58** 229
- [5] Jaeger N I, Möller K and Plath P J 1986 *J. Chem. Soc. Faraday Trans. I* **82** 3315  
Plath P J 1988 *Catal. Today* **3** 475  
Plath P J, Möller K and Jaeger N I 1988 *J. Chem. Soc. Faraday Trans. I* **84** 1751
- [6] Essam J W 1989 *J. Phys. A: Math. Gen.* **22** 4927
- [7] Essam J W and Tanlakishani W 1987 *Disorder in Physical Systems* ed G R Grimmett and D J A Welsh (Oxford: Oxford University Press)
- [8] Martins M L, Verona de Resende H F, Tsallis C and de Magalhães A C N 1991 *Phys. Rev. Lett.* **66** 2045
- [9] Kohring G A and Schreckenberg M 1992 *J. Physique* **2** 2033
- [10] Tomé T 1993 private communication
- [11] Carter J A 1992 private communication